Freestanding Graphene Paper Supported Three-Dimensional Porous Graphene–Polyaniline Nanocomposite Synthesized by Inkjet Printing and in Flexible All-Solid-State Supercapacitor

Article *in* ACS Applied Materials & Interfaces · September 2014

DOI: 10.1021/am504539k · Source: PubMed

7 authors, including:

Zheye Zhang
Huazhong University of Science and Technology
17 PUBLICATIONS **339** CITATIONS
SEE PROFILE

Jiangbo Xi
Chinese Academy of Sciences
14 PUBLICATIONS **114** CITATIONS
SEE PROFILE

Yongan Huang
Huazhong University of Science and Technology
61 PUBLICATIONS **411** CITATIONS
SEE PROFILE

Shuai Wang
Huazhong University of Science and Technology
115 PUBLICATIONS **1,861** CITATIONS
SEE PROFILE

ACS APPLIED MATERIALS & INTERFACES

Research Article

www.acsami.org

Freestanding Graphene Paper Supported Three-Dimensional Porous Graphene–Polyaniline Nanocomposite Synthesized by Inkjet Printing and in Flexible All-Solid-State Supercapacitor

Kai Chi,[†,⊥] Zheye Zhang,[†,⊥] Jiangbo Xi,[†,⊥] Yongan Huang,[‡] Fei Xiao,*[,†] Shuai Wang,*[,†] and Yunqi Liu[§]

[†]School of Chemistry & Chemical Engineering, Huazhong University of Science and Technology, Wuhan 430074, People's Republic of China

[‡]State Key Lab of Digital Manufacturing Equipment and Technology, School of Mechanical Science and Engineering, Huazhong University of Science and Technology, Wuhan 430074, People's Republic of China

[§]Beijing National Laboratory for Molecular Sciences, Institute of Chemistry, Chinese Academy of Sciences, Beijing 100190, People's Republic of China

Supporting Information

ABSTRACT: Freestanding paper-like electrode materials have trigged significant research interest for their practical application in flexible and lightweight energy storage devices. In this work, we reported a new type of flexible nanohybrid paper electrode based on full inkjet printing synthesis of a freestanding graphene paper (GP) supported three-dimensional (3D) porous graphene hydrogel (GH)–polyaniline (PANI) nanocomposite, and explored its practical application in flexible all-solid-state supercapacitor (SC). The utilization of 3D porous GH scaffold to load nanostructured PANI dramatically enhances the electrical conductivity, the specific capacitance and the cycle stability of the GH–PANI nanocomposite. Additionally, GP can intimately interact with GH–PANI through π–π stacking to form a unique freestanding GP supported GH–PANI nanocomposite (GH–PANI/GP) with distinguishing mechanical, electrochemical and capacitive properties. These exceptional attributes, coupled with the merits of full inkjet printing strategy, lead to the formation of a high-performance binder-free paper electrode for flexible and lightweight SC application. The flexible all-solid-state symmetric SC based on GH–PANI/GP electrode and gel electrolyte exhibits remarkable mechanical flexibility, high cycling performance and acceptable energy density of 24.02 Wh kg^{-1} at a power density of 400.33 W kg^{-1}. More importantly, the proposed simple and scale-up full inkjet printing procedure for the preparation of freestanding GP supported 3D porous GH-PANI nanocomposite is a modular approach to fabricate other graphene-based nanohybrid papers with tailorable properties and optimal components.

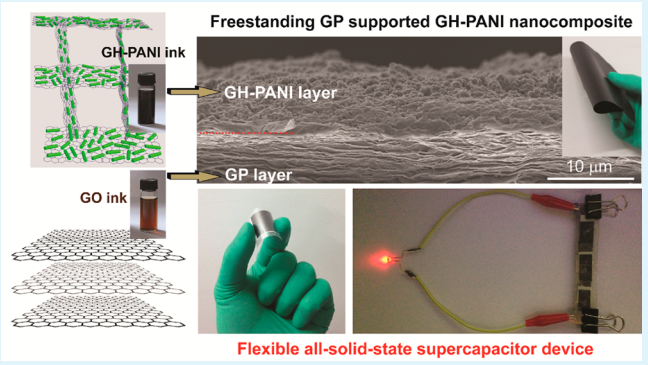

KEYWORDS: *freestanding graphene paper, three-dimensional porous graphene–polyaniline nanocomposite, full inkjet printing synthesis, flexible electrode, all-solid-state supercapacitor*

1. INTRODUCTION

Over the past few years, there has been significant interest in the development of flexible and lightweight energy storage devices for their practical applications ranging from flexible/bendable electronic equipment to microelectromechanical systems. Especially, the flexible supercapacitor (SC) has attracted significant attention due to its large power density, moderate energy density, good operational safety and long cycling life.[1−6] For the fabrication of a flexible SC, freestanding binder-free electrodes with a rational structure design and optimal composite play a large part in the capacitive performance of the device. Two-dimensional (2D) graphene nanosheets have been of considerable current interest in SC application for their high electrical conductivity (10^3–10^4 S m^{-1}) and huge specific surface area (calculated theoretical value = 2630 m^2 g^{-1}).[7−9] Recent studies by several groups including us have shown that graphene-based paper-like structures demonstrate unique electronic, mechanical and chemical properties such as high electrical conductivity, flexibility, high mechanical strength and chemical stability, making them an intriguing candidate for a flexible SC.[10−16]

The freestanding graphene paper (GP) can be prepared by various methods including vacuum filtering, self-assembly and pressing graphene aerogel or hydrogel.[17−20] However, these methods share a common challenge to develop large-scale electrode materials, which limits their practical applications in

Received: July 11, 2014
Accepted: September 2, 2014
Published: September 2, 2014

commercial energy storage devices. To address this challenge, tremendous efforts have been devoted to developing some advanced technologies, such as inkjet printing, to fabricate graphene film and graphene-based functional devices.[21] The printing technique through well-controlled ejection of graphene ink droplets from nozzles onto various substrates not only provides the capability of printing films in controlled geometries and at specific locations on various substrates but also enables the manufacture of large-area flexible devices at low cost.[22,23] Nevertheless, for SC application, the GP materials still suffer from a severe drawback: the graphene nanosheets tend to restack themselves during the formation of freestanding paper structure, which is detrimental for the accessibility to the electrolyte and the formation of electrical double-layer charges. Jang's group presented a significant improvement on graphene-based materials for SC. They prepared curved graphene sheets that were not restacking face to face, which made full utilization of the highest intrinsic surface capacitance and specific surface area of single-layer graphene. The curved morphology also facilitated the formation of mesopores accessible to and wettable by ionic liquids electrolyte. These advantages enabled the as-obtained SC with a high voltage (e.g., 4 V) and an unprecedented level of nearly 90 Wh/kg at a current density of 1 A/g at room temperature and a level of 136 Wh/kg at 80 °C.[24] Recently, three-dimensional (3D) graphene hydrogel (GH) self-assembled from graphene oxide (GO) through the $\pi-\pi$ stacking has also attracted tremendous attention for its excellent mechanical, thermal and electrochemical properties.[25,26] Especially, the macro-assembled GH possesses high wettability, rich macro/mesoporosity, large surface area and multidimensional conductivity, which provides more conductive channels to facilitate the access of the aqueous ions onto the graphene surface, and therefore holds great promise for SC application.[27]

In this work, we have developed a 3D GH loaded polyaniline (PANI) nanomaterial (GH–PANI), and then coated it on freestanding GP to fabricate a new type of flexible nanohybrid paper electrode by well-controlled full inkjet printing method. PANI is a highly promising electrode material for a SC due to its low cost, environmental stability and high theoretical specific pseudocapacitance.[28] However, it suffers from several disadvantages such as moderate electrical conductivity[29] and poor cycling stability caused by swelling and shrinkage during the doping and dedoping process.[30] The incorporations of PANI in graphene-based material to fabricate flexible graphene/PANI nanofiber composite films[14] and freestanding hierarchical carbon nanofiber/GO/PANI films[15] have been demonstrated to be an effective strategy to enhance the electrical conductivity and stability of PANI. Our results also show that GH with multidimensional conductivity, large surface area and excellent mechanical/chemical stability is an ideal scaffold to load nanostructured PANI as well as enhance the electrical conductivity and stability of the resultant GH–PANI nanocomposite. As illustrated in Scheme 1, the homogeneous GH–PANI ink was obtained by ball milling and ultrasonic treatment of GH–PANI nanomaterial. The proposed GP supported 3D GH–PANI nanocomposite (GH–PANI/GP) was prepared by printing graphene oxide (GO) ink on a commercial paper, followed by overprinting the GH–PANI inks on it. The rough surface of GP can intimately interact with the GH–PANI nanocomposite through the $\pi-\pi$ stacking. After reduced by hydroiodic acid (HI) and simultaneous peeling off from the commercial paper substrate, the freestanding GH–PANI/GP

Scheme 1. Schematic Illustration of the Fabrication Process of GH–PANI/GP[a]

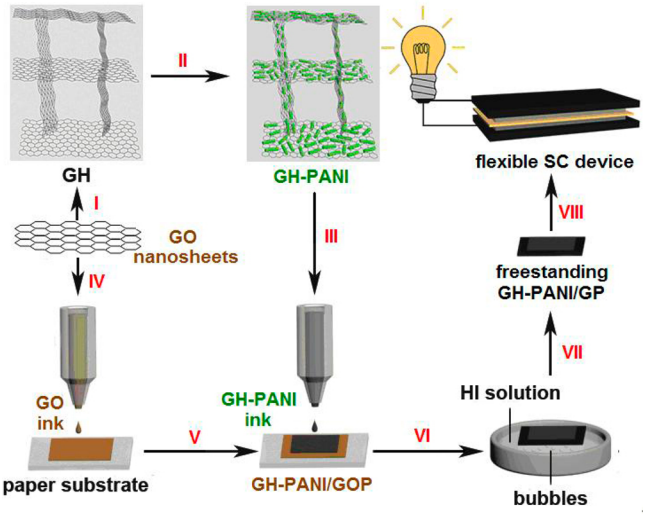

[a] (Step I) Self-assembly of GO nanosheets into 3D GH. (Step II) In-situ polymerization of PANI on GH. (Step III) Ball milling and ultrasonic treatment of 3D GH–PANI composite to form GH–PANI ink. (Step IV) Printing GO ink on paper substrate to form GOP; (Step V) Overprinting the GH–PANI inks on GOP; (Step VI) Soaking GH–PANI/GOP in the HI solution. (Step VII) Simultaneous reducing GH–PANI/GOP by HI and peeling it off from the commercial paper substrate to form freestanding GH–PANI/GP. (Step VIII) Fabrication of flexible SC device based on GH–PANI/GP electrode and gel electrolyte.

can be obtained. Owing to the synergistic effect of different components in the as-prepared nanohybrid paper, the flexible and lightweight all-solid-state symmetric SC based on GH–PANI/GP electrode exhibits acceptable energy density, remarkable flexibility and high cycling performance. The maximum energy density of 24.02 Wh kg^{-1} (at a power density of 400.33 W kg^{-1}) and power density of 3202.4 W kg^{-1} (at an energy density of 13.29 Wh kg^{-1}) can be achieved at an operating voltage of 0.8 V. This opens a new possibility to develop high-performance flexible energy-related device and wearable electronics.

2. EXPERIMENTAL SECTION

2.1. Preparation of Ink Sample. GO was synthesized from graphite powder based on the modified Hummer's method.[31] The concentration of the prepared GO solution was about 10 mg mL^{-1}. GH was prepared by hydrothermal treatment of prepared GO solution using the procedure reported previously.[26,32] For the synthesis of the GH–PANI nanocomposite, the macroscopic GH was immersed into 40 mL of 0.5 M H_2SO_4 solution containing 0.32 mL aniline monomer overnight. Then, 40 mL of 0.5 M H_2SO_4(aq) containing 750 mg ammonium peroxydisulfate was added into the above mixture. After reaction at 60 °C for 2 h, the GH was taken out and washed with H_2SO_4 solution, ethanol, ammonia and distilled water subsequently. The as-prepared GH–PANI nanocomposite was added to an agate capsule containing agate balls of 5 mm in diameter. The container was then fixed in the planetary ball-mill machine and agitated with 500 rpm for 30 min. After ball milling and dispersion in a water and ethanol mixture (volume ratio is 1:1) upon ultrasonic treatment, the homogeneous GH–PANI inks can be obtained. The PANI ink was prepared during the same procedure but without the addition of GH.

2.2. Preparation of Freestanding Nanohybrid Paper. A commercial Dimatix Materials Printer (DMP 2800, Dimatix-Fujifilm Inc.) was used to print the GO and GH–PANI inks (concentration of

2 mg mL^{-1} in water, droplet size = 10 pL). GO ink was first printed on commercial paper to form GO paper (GOP). Then, the GH−PANI ink was overprinted on GOP substrate. For the preparation of PANI/GOP, the PANI ink was directly printed on the GOP substrate. The as-obtained GH−PANI/GOP and PANI/GOP were reduced to GH−PANI/GP and PANI/GP by soaking GH−PANI/GOP and PANI/GOP in the HI solution (45 wt %) for 1 h at room temperature, the CO_2 bubbles generated from the cellulose papers prompt the thin film peeling off the paper in a self-releasing way.

2.3. Characterization. The morphology and structure of the as-prepared papers were characterized with a field-emission scanning electron microscopy (SEM, FEI, Nova NanoSEM 450). X-ray photoelectron spectroscopy (XPS) measurements were performed on a Kratos-Axis spectrometer with monochromatic Al Kα (1486.71 eV) X-ray radiation (15 kV and 10 mA) and a hemispherical electron energy analyzer. X-ray powder diffraction (XRD) patterns were recorded using a diffractometer (X′ Pert PRO, Panalytical B.V., Netherlands) equipped with a Cu Kα radiation source (λ = 1.5406 Å). Raman spectra were measured on a confocal laser micro-Raman spectrometer (Thermo Fischer DXR, USA) equipped with a He−Ne laser of excitation of 532 nm. The weight of the electrode materials was measured by electronic balance. The conductivity of the as-prepared GP and GH−PANI/GP was measured by the four-probe method.

2.4. Electrochemical Measurement. All the electrochemical measurements were performed with a CHI 760E electrochemical workstation (CH Instruments Inc., USA). For single electrode tests, a three-electrode set up in 1.0 M H_2SO_4 was used, with gauze platinum and saturated calomel electrode (SCE) as a counter and reference electrode, respectively. To fabricate the all-solid-state symmetric SC device, the gel electrolyte was first prepared by mixing 6 g of H_2SO_4 and 6 g of poly(vinyl alcohol) (PVA) in 60 mL of deionized water and heated to 85 °C under vigorous stirring until the solution became clear. Next, two pieces of GH−PANI/GP were immersed into the PVA/H_2SO_4 gel electrolyte for 5 min and then taken out and assembled together with a cellulose separator sandwiched in between the two electrodes. The device was finally solidified at room temperature to vaporize the excess water.

3. RESULTS AND DISCUSSION

Figure 1 shows the photographs of different graphene-based inks and macroscopic nanohybrid paper materials. GO

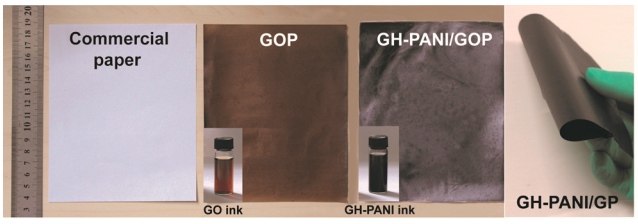

Figure 1. Photographs of different graphene-based inks and macroscopic nanohybrid paper materials.

nanosheets prepared by Hummer's method have abundant polar surface functional groups and therefore are highly dispersible in aqueous medium, which enables them to be used as an ink material for inkjet printing. The resultant GO ink was then printed on commercial paper via a facile and scale-up inkjet printing method to form GOP, which can be converted to freestanding GP by chemical reduction using HI and simultaneously peeled off from paper substrate in a self-releasing way. The obtained GP exhibits high electrical conductivity (13.5 Ω sq^{-1}), lightweight (1.2 mg cm^{-2}) and excellent mechanical flexibility, making it an intriguing candidate to support the 3D GH−PANI nanocomposite. For the preparation of the GH−PANI ink material, the 3D porous GH was first synthesized by hydrothermal treatment of GO solution and then acted as a scaffold to host PANI nanomaterial. After ball milling and dispersion in a water and ethanol mixture upon ultrasonic treatment, the homogeneous GH−PANI ink was obtained. The as-prepared GH−PANI ink could be overprinted on a GO paper substrate to form the GH−PANI/GOP, upon which the dark yellow-colored GO paper turned black. The proposed freestanding GH−PANI/GP was also obtained by chemical reduction using HI and peeling off from paper substrate, its electrical conductivity was measured to be 18 Ω sq^{-1}. Compared with the general strategies using graphene/PANI powdery materials (can not meet the requirements of flexible binder-free electrode),[33,34] vacuum filtrating mixtures of graphene sheets and prepared PANI nanobers (lack of truly synergistic effect of the PANI and graphene nanosheets)[35] and the electropolymerization of aniline monomers on GP (unsuitable for large-scale and cost-reasonable production),[36,37] our full inkjet printing techniques combined with followed chemical reduction and self-releasing way offer several advantages in term of simple, efficient and low-cost to produce large-area flexible and lightweight graphene−PANI nanohybrid paper.

The SEM images of the GH and GH−PANI nanocomposites are shown in Figure 2a−d. GH exhibits a well-defined and interconnected 3D porous network driven by $\pi-\pi$ stacking interactions of graphene nanosheets (Figure 2a), from which a number of hierarchical pores with a wide size distribution were observed (Figure 2b). The coral-like PANI nanostructures are highly loaded on the pore wall of GH by in situ chemical polymerization of the aniline monomer, as shown in Figure 2c. A high-resolution image reveals that the coral-like PANI nanostructures consist of numerous interconnected nanorods. The average diameter and length of PANI nanorods are measured to be approximately 80 and 400 nm, respectively (Figure 2d). After a thin layer of GH−PANI nanocomposite is printed on GP, the layered stacking of GP and porous GH−PANI thin film are clearly observed in Figure 2e−g, where the GH−PANI layer has been well coated on the surface of GP to form a tightly compact structure.

Figure 3a,b shows the XPS spectra of deconvoluted C 1s in GOP and GP samples. The deconvoluted C 1s in GP displays a predominant peak associated with C═C/C—C (284.4 eV), and relative weak peaks attributed to C—O (285.6 eV) and C═O (288.0 eV), respectively, different from two main carbon bonds of C═C/C—C and C—O in the original GOP sample. The significant decrease signal of the oxygen-containing groups in GP demonstrates a high degree of deoxygenating and successful reduction of GOP to GP during the chemical reduction process, which effectively increases the electrical conductivity of GP. Figure 3c exhibits the XRD patterns of GOP and GP samples. The GOP exhibits one sharp peak centered at 10.5°, corresponding to the (002) reflection of stacked GO sheets with an interlayer spacing of 8.42 Å. After reduction, the peak position of GP shifts from 10.5° to 24.1° and the interlayer spacing decreases to 3.69 Å, further confirming the removal of oxygen-containing groups on GO nanosheets. The surface compositions of GP and GH−PANI/GP are further characterized by Raman spectroscopy. GP displays two prominent peaks at 1355 and 1595 cm^{-1}, corresponding to the well-documented D and G bands, respectively. For GH−PANI/GP, three new representative peaks arising from PANI can be indexed at 989, 1168 and 1496

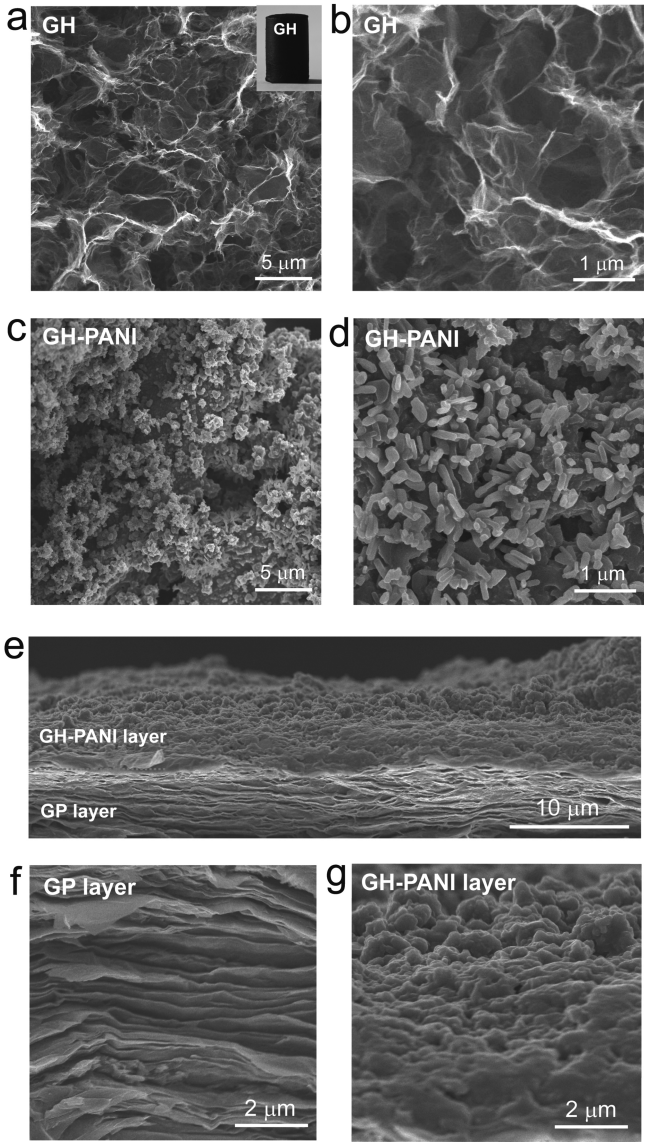

Figure 2. SEM images of (a, b) GH and (c, d) GH−PANI at different magnification. Cross-section view of (e) GH−PANI/GP at low magnification. Cross-section view of (f) GP layer and (g) GH−PANI layer on GH−PANI/GP at high magnification.

cm^{-1} (Figure 3d), assigned to the C—H deformation out-of-plane of the benzenoid ring, C—H bending vibration in the benzenoid ring and C═N stretching deformation of the quinonoid units, respectively.[38]

To explore the advantages of flexible and lightweight GH−PANI/GP for SC application, the GH−PANI/GP has been used as the working electrode in three-electrode system to evaluate its electrochemical properties. Figure 4a shows the cyclic voltammetry (CV) curves of the GH−PANI/GP electrode, which exhibits nearly rectangular shapes at different scan rates from 10 to 200 mV s^{-1}, indicating that GH−PANI/GP processes low resistance and ideal supercapacitive properties. Furthermore, two couples of redox peaks are also observed from the CV curves, which attribute to the leucoemeraldine/emeraldine and emeraldine/pernigraniline transitions of PANI.[39] Figure 4b,c displays the galvanostatic (GA) charge/discharge curves of GH−PANI/GP electrode at different current densities. The discharge curves are almost symmetrical to the corresponding charge curves, indicating the pseudocapacitive contribution along with the double layer contribution.

The mass specific capacitances and the areal specific capacitances are calculated from the GA charge/discharge curves. As shown in Figure 4d, the mass specific capacitance GH−PANI/GP achieves is as high as 864 F g^{-1} at a current density of 1 A g^{-1}, and the areal capacitance of GH−PANI/GP corresponds to 190.6 mF cm^{-2} at a current density of 0.5 mA cm^{-2}. About 53% and 50.2% of capacitance is retained when the current density increases to 8 A g^{-1} and 2.5 mA cm^{-2}, respectively. The capacitance values of GH−PANI/GP are much better than the values reported for other graphene/PANI nanocomposites.[33−37,40,41] Moreover, take into account that the stability is crucial for SCs operation; the cycling stability of GH−PANI/GP has been tested along with controlled PANI/GP by repeating the GV test in the voltage window from 0 to 0.8 V at a current density of 8 A g^{-1}. The results show that the GH−PANI/GP electrode exhibits excellent cycling stability. Its specific capacitance preserves 96% after 1000 cycles. In comparison, PANI/GP shows 63.7% capacitance retention over 1000 cycles (Supporting Information, Figure S1). This indicates that the incorporation of pseudocapacitive PANI into the GH scaffold effectively improves the cycle performance of the resultant nanohybrid electrode. The remarkable improved electrochemical capacitive activity and cycle stability of GH−PANI/GP can be recognized as (i) nanoscale PANI in situ grown on GH scaffold provides direct and stable pathways for rapid electron transport and enhanced specific capacitance originated from the good pseudocapacity of PANI; (ii) GH scaffold serves as a robust 3D substrate to immobilize active PANI nanorods, which provides multidimensional surface contact for PANI nanomaterials and endows the structural integrity of PANI on it, and therefore prevents the loss of active materials due to their structure or volume changes during redox reactions; (iii) GH scaffold with continuously conductive reticulation and high wettability promotes good access of electrolyte to the active GH−PANI nanocomposite, leading to a low charge transfer resistance and improved supercapacitive properties of the resultant electrode; (iv) direct printing GH−PANI ink on freestanding GP ensures good mechanical adhesion and electric connection of the active GH−PANI nanomaterial to the current collector; therefore, the specific capacitances of GH−PANI/GP are well maintained after 1000 cycles. Furthermore, this unique electrode design avoids the use of binder and conducting additives, which improves the utilization of the electrode material that contributes to the total capacitance.

The flexible all-solid-state symmetric SC device can be assembled with two pieces of GH−PANI/GP using PVA/H_3PO_4 as the gel electrolyte. The CV curves for a single symmetric device maintain the quasirectangular shape at all scan rates from 10 to 200 mV s^{-1} (Figure 5a). The GA charge/discharge curves of the device shown in Figure 5b display a straight line and symmetric shape within a 0.8 V potential window at different current densities from 1 to 8 A g^{-1}. These characteristics suggest an ideal capacitance of the symmetric device. In addition, the electrochemical impedance spectroscopy (EIS) measurement has been performed to study the electrochemical performances of the device. The Nyquist plots demonstrate almost vertical line in a low-frequency region (Figure 5c), indicating a nearly ideal capacitive behavior. At the high frequency region, the equivalent series resistances (ESRs) of the device are measured to be about 0.36 Ω by extrapolating

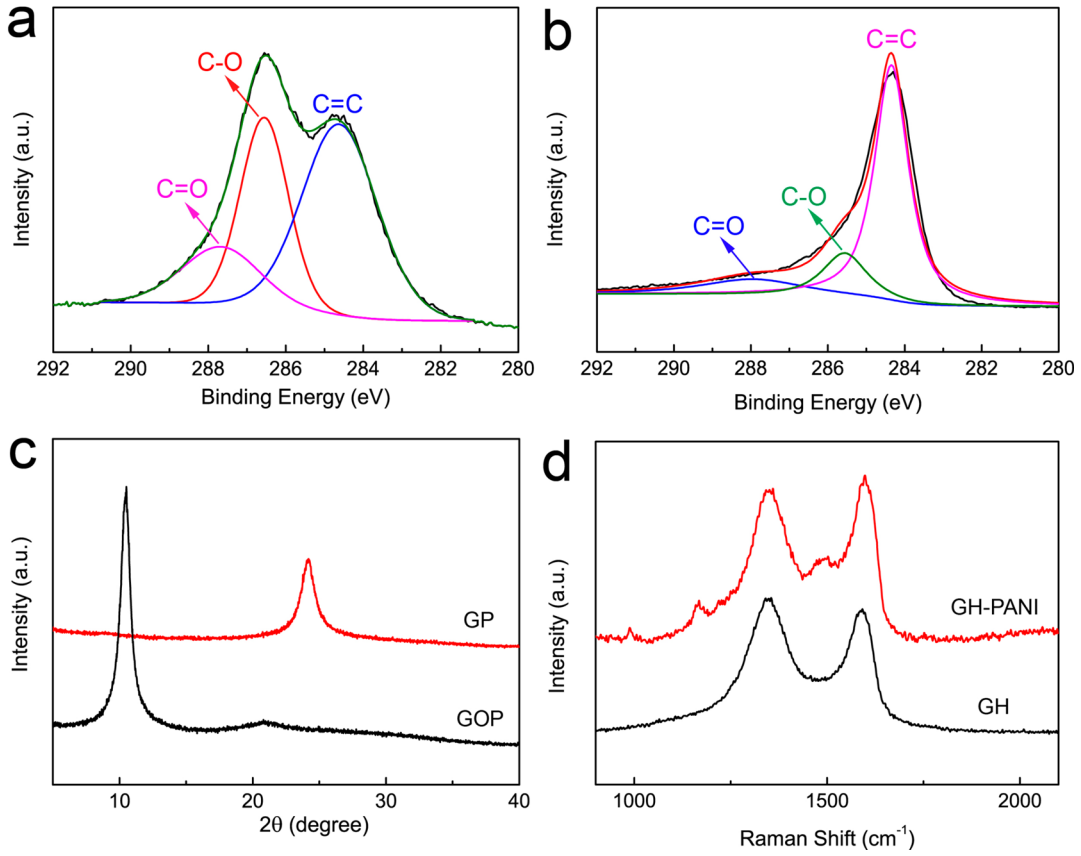

Figure 3. Deconvoluted C 1s spectra of (a) GOP and (b) GP. (c) XRD patterns of GOP and GP. (d) Raman spectra of GH and GH−PANI nanocomposites.

the straight line to intersect the real axis. The low ESR and R_{ct} values indicate that GP can indeed act as a conductive substrate as well as current collector for intimately loading of GH−PANI nanocomposites. The energy and power densities for the symmetric device are calculated from the GA charge/discharge curves and plotted on the Ragone diagram. As shown in Figure 5d, the maximum energy density of 24.02 Wh kg^{-1} (at a power density of 400.33 W kg^{-1}) and power density of 3202.4 W kg^{-1} (at a energy density of 13.29 Wh kg^{-1}) can be achieved at an operating voltage of 0.8 V. The energy density in this work is higher than those of many previously reported devices,[42−46] which is contributed fromm the synergistic effect of different components in the GH−PANI/GP composite materials.

Figure 5e shows the influence of the bending-induced mechanical stress upon the capacitance retention. Upon bending inward to angles of 45°, 90° and 180°, the symmetric device exhibits only 1% decrease of the capacitance. And the change of the capacitance is less than 2% after 180° bending for 100 times. Figure 5e inset shows that upon bending inward to different angles and 180° bending for 100 times, the CV curves still remain their original shape. These demonstrate that the change of electrochemical performance of the flexible SC is negligible under different bending angles and bending times. The cycling stability of the SC has been tested through a cyclic charge/discharge process at a fixed current density of 8 A g^{-1}. As displayed in Figure 5f, the symmetric device still retains 85.6% of the initial capacitance after 5000 cycles, demonstrative of its excellent long-term cycling stability. This can be ascribed to the unique electrode design of freestanding GH−PAN/GP. 3D porous GH can act as an efficient scaffold to support PANI nanomaterials and avoid their loss during the process of numerous charge−discharge cycles. Additionally, the GH−PAN/GP obtained by full inkjet printing synthesis can keep the structural integrity and mechanical stability of electrode materials during the cycling tests, which therefore improve the cycling performance of the assembled device. Furthermore, three symmetric devices connected in series can light up a red light emitting diode (Figure 5f inset), which reveals its practical application in energy storage.

4. CONCLUSION

In summary, we developed a facile and scale-up printing method to fabricate a new type of flexible and lightweight paper electrode, i.e., freestanding GP supported 3D GH−PANI nanocomposite, and explored its practical application in a flexible all-solid-state symmetric SC. Owing to the synergistic effects of different components in GH−PANI/GP composite material and the merits of the full inkjet printing synthesis strategy, the all-solid-state symmetric SC device based on binder-free GH−PANI/GP electrode and gel electrolyte exhibits acceptable energy density, remarkable flexibility and high cycling performance. We anticipate that our strategy can provide a significant step forward to bringing graphene-based nanohybrid paper materials to diverse applications in flexible lithium ion batteries, supercapacitor, solar cells, biosensor, bioengineering and other electronic systems.

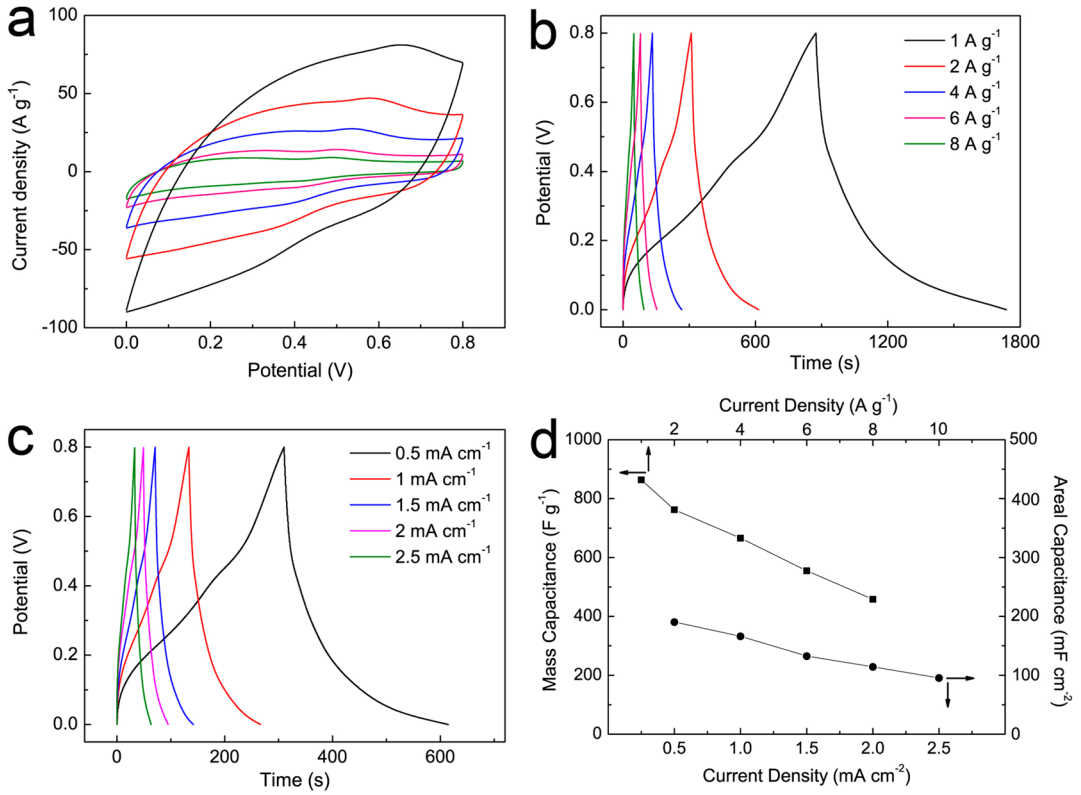

Figure 4. (a) CV curves for GH−PANI/GP electrode at different scan rates (10, 20, 50, 100 and 200 mV s^{-1}) in 1.0 M H_2SO_4 electrolyte. (b, c) GA charge/discharge curves of GH−PANI/GP electrode at different current densities (1, 2, 4, 6 and 8 A g^{-1}). (d) Mass and areal capacitance calculated from the charge/discharge curves as a function of current density.

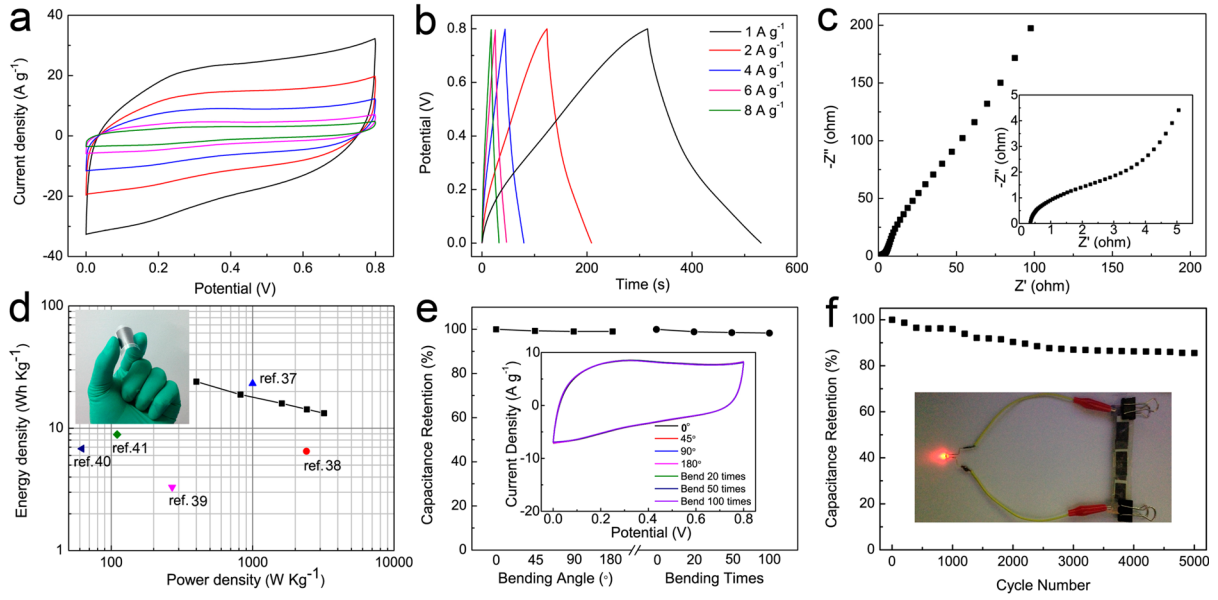

Figure 5. (a) CV and (b) GA charge−discharge curves of the all-solid-state symmetric SC. (c) Nyquist plot of the all-solid-state device. (d) Ragone plots of the SC device compared with data in other literature. (e) Capacitance retention ratio of the flexible SC device after bending inward to different angles or being bent repeatedly (bending angle and number of times indicated). (f) Cycling behavior of the SC device at a current density of 8 A g^{-1}.

■ ASSOCIATED CONTENT

Supporting Information

Cycling behavior of GH-PANI/GP and PANI/GP electrodes at a current density of 8 A g^{-1}. This material is available free of charge via the Internet at http://pubs.acs.org.

■ AUTHOR INFORMATION

Corresponding Authors

*S. Wang. E-mail: chmsamuel@mail.hust.edu.cn.
*F. Xiao. E-mail: xiaofei@hust.edu.cn.

Author Contributions

[⊥]These authors contributed equally.

Notes

The authors declare no competing financial interest.

■ ACKNOWLEDGMENTS

This research was financially supported by the National Natural Science Foundation of China (Project No. 51173055 and No. 21305048), and National Program on Key Basic Research Project (973 Program, Grant No. 2013CBA01600)

■ REFERENCES

(1) Simon, P.; Gogotsi, Y. Materials for Electrochemical Capacitors. *Nat. Mater.* **2008**, *7*, 845−854.
(2) Fu, Y. P.; Cai, X.; Wu, H. W.; Lv, Z. B.; Hou, S. C.; Peng, M.; Yu, X.; Zou, D. C. Fiber Supercapacitors Utilizing Pen Ink for Flexible/Wearable Energy Storage. *Adv. Mater.* **2012**, *24*, 5713−5718.
(3) Yu, G. H.; Hu, L. B.; Liu, N.; Wang, H. L.; Vosgueritchian, M.; Yang, Y.; Cui, Y.; Bao, Z. N. Enhancing the Supercapacitor Performance of Graphene/MnO_2 Nanostructured Electrodes by Conductive Wrapping. *Nano Lett.* **2011**, *11*, 4438−4442.
(4) Huang, H. F.; Tang, Y. M.; Xu, L. Q.; Tang, S. L.; Du, Y. W. Direct Formation of Reduced Graphene Oxide and 3D Lightweight Nickel Network Composite Foam by Hydrohalic Acids and Its Application for High-Performance Supercapacitors. *ACS Appl. Mater. Interfaces* **2014**, *6*, 10248−10257.
(5) Huang, L.; Li, C.; Shi, G. Q. High-Performance and Flexible Electrochemical Capacitors Based on Graphene/Polymer Composite Films. *J. Mater. Chem. A* **2014**, *2*, 968−974.
(6) Li, Y. R.; Sheng, K. X.; Yuan, W. J.; Shi, G. Q. A High-Performance Flexible Fibre-Shaped Electrochemical Capacitor Based on Electrochemically Reduced Graphene Oxide. *Chem. Commun.* **2013**, *49*, 291−293.
(7) Novoselov, K. S.; Geim, A. K.; Morozov, S. V.; Jiang, D.; Zhang, Y.; Dubonos, S. V.; Grigorieva, I. V.; Firsov, A. A. Electric Field Effect in Atomically Thin Carbon Films. *Science* **2004**, *306*, 666−669.
(8) Stankovich, S.; Dikin, D. A.; Dommett, G. H. B.; Kohlhaas, K. M.; Zimney, E. J.; Stach, E. A.; Piner, R. D.; Nguyen, S. 15. T.; Ruoff, R. D. Graphene-based Composite Materials. *Nature* **2006**, *442*, 282−286.
(9) Geim, A. K. Graphene: Status and Prospects. *Science* **2009**, *324*, 1530−1534.
(10) EI-Kady, M. F.; Strong, V.; Dubin, S.; Kaner, R. B. Laser Scribing of High-Performance and Flexible Graphene-based Electrochemical Capacitors. *Science* **2012**, *335*, 1326−1330.
(11) Stoller, M. D.; Park, S. J.; Zhu, Y.; An, J.; Ruoff, R. S. Graphene-based Ultracapacitors. *Nano Lett.* **2008**, *8*, 3498−3502.
(12) Xiao, F.; Song, J. B.; Gao, H. C.; Zan, X.; Xu, R.; Duan, H. W. Coating Graphene Paper with 2D-Assembly of Electrocatalytic Nanoparticles: A Modular Approach toward High-Performance Flexible Electrodes. *ACS Nano* **2012**, *6*, 100−110.
(13) Xiao, F.; Li, Y.; Zan, X.; Liao, K.; Xu, R.; Duan, H. W. Growth of Metal−Metal Oxide Nanostructures on Freestanding Graphene Paper for Flexible Biosensors. *Adv. Funct. Mater.* **2012**, *22*, 2487−2494.
(14) Wu, Q.; Xu, Y. X.; Yao, Z. Y.; Liu, A. R.; Shi, G. Q. Supercapacitors Based on Flexible Graphene/Polyaniline Nanofiber Composite Films. *ACS Nano* **2010**, *4*, 1963−1970.
(15) Xu, D. D.; Xu, Q.; Wang, K. X.; Chen, J.; Chen, Z. M. Fabrication of Free-Standing Hierarchical Carbon Nanofiber/Graphene Oxide/Polyaniline Films for Supercapacitors. *ACS Appl. Mater. Interfaces* **2014**, *6*, 200−209.
(16) Chen, J.; Li, C.; Shi, G. Q. Graphene Materials for Electrochemical Capacitors. *J. Phys. Chem. Lett.* **2013**, *4*, 1244−1253.
(17) Zhang, L. L.; Zhao, X.; Stoller, M. D.; Zhu, Y. W.; Ji, H. X.; Murali, S.; Wu, Y. P.; Perales, S.; Clevenger, B.; Ruoff, R. S. Highly Conductive and Porous Activated Reduced Graphene Oxide Films for High Power Supercapacitors. *Nano Lett.* **2012**, *12*, 1806−1812.
(18) Chen, C. M.; Yang, Q. H.; Yang, Y. G.; Lv, W.; Wen, Y. F.; Hou, P. X.; Wang, M. Z.; Cheng, H. M. Self-Assembled Free-Standing Graphite Oxide Membrane. *Adv. Mater.* **2009**, *21*, 3007−3011.
(19) Liu, F.; Song, S.; Xue, D.; Zhang, H. Folded Structured Graphene Paper for High Performance Electrode Materials. *Adv. Mater.* **2012**, *24*, 1089−1094.
(20) Xu, Y. X.; Lin, Z. Y.; Huang, X. Q.; Liu, Y.; Huang, Y.; Duan, X. F. Flexible Solid-State Supercapacitors Based on Three-Dimensional Graphene Hydrogel Films. *ACS Nano* **2013**, *7*, 4042−4049.
(21) Gates, B. D. Flexible Electronics. *Science* **2009**, *323*, 1566−1567.
(22) Minemawari, H.; Yamada, T.; Matsui, H.; Tsutsumi, J. Y.; Haas, S.; Chiba, R.; Kumai, R.; Hasegawa, T. Inkjet Printing of Single-Crystal Films. *Nature* **2011**, *475*, 364−367.
(23) Li, J. T.; Ye, F.; Vaziri, S.; Muhammed, M.; Lemme, M. C.; Östling, M. Efficient Inkjet Printing of Graphene. *Adv. Mater.* **2013**, *25*, 3985−3992.
(24) Liu, C.; Yu, Z.; Neff, D.; Zhamu, A.; Jang, B. Z. Graphene-based Supercapacitor with an Ultrahigh Energy Density. *Nano Lett.* **2010**, *10*, 4863−4868.
(25) Cong, H. P.; Ren, X. C.; Wang, P.; Yu, S. H. Macroscopic Multifunctional Graphene-based Hydrogels and Aerogels by a Metal Ion Induced Self-Assembly Process. *ACS Nano* **2012**, *6*, 2693−2703.
(26) Xu, Y. X.; Sheng, K. X.; Li, C.; Shi, G. Q. Self-Assembled Graphene Hydrogel via a One-Step Hydrothermal Process. *ACS Nano* **2010**, *4*, 4324−4330.
(27) Zhang, L.; Shi, G. Q. Preparation of Highly Conductive Graphene Hydrogels for Fabricating Supercapacitors with High Rate Capability. *J. Phys. Chem. C* **2011**, *115*, 17206−1721.
(28) Zhou, Y.; Qin, Z. Y.; Li, L.; Zhang, Y.; Wei, Y. L.; Wang, L. F.; Zhu, M. F. Polyaniline/Multi-Walled Carbon Nanotube Composites with Core−Shell Structures as Supercapacitor Electrode Materials. *Electrochim. Acta* **2010**, *55*, 3904−3908.
(29) Zhang, J.; Zhao, X. S. Conducting Polymers Directly Coated on Reduced Graphene Oxide Sheets as High-Performance Supercapacitor Electrodes. *J. Phys. Chem. C* **2012**, *116*, 5420−5426.
(30) Frackowiak, E.; Khomenko, V.; Jurewicz, K.; Lota, K.; Eguin, F. B. Supercapacitors Based on Conducting Polymers/Nanotubes Composites. *J. Power Sources* **2006**, *153*, 413−418.
(31) Hummers, W. S.; Offeman, R. E. Preparation of Graphitic Oxide. *J. Am. Chem. Soc.* **1958**, *80*, 1339−1339.
(32) Zhang, Z. Y.; Xiao, F.; Guo, Y. L.; Wang, S.; Liu, Y. Q. One-Pot Self-Assembled Three-Dimensional TiO_2-Graphene Hydrogel with Improved Adsorption Capacities and Photocatalytic and Electrochemical Activities. *ACS Appl. Mater. Interfaces* **2013**, *5*, 2227−2233.
(33) Xu, J.; Wang, K.; Zu, S. Z.; Han, B. H.; Wei, Z. Hierarchical Nanocomposites of Polyaniline Nanowire Arrays on Graphene Oxide Sheets with Synergistic Effect for Energy Storage. *ACS Nano* **2010**, *4*, 5019−5026.
(34) Kumar, N. A.; Choi, H. J.; Shin, Y. R.; Chang, D. W.; Dai, L.; Baek, J. B. Polyaniline-Grafted Reduced Graphene Oxide for Efficient Electrochemical Supercapacitors. *ACS Nano* **2012**, *6*, 1715−1723.
(35) Wu, Q.; Xu, Y. X.; Yao, Z. Y.; Liu, A. R.; Shi, G. Q. Supercapacitors Based on Flexible Graphene/Polyaniline Nanofiber Composite Films. *ACS Nano* **2010**, *4*, 1963−1970.
(36) Wang, D. W.; Li, F.; Zhao, J. P.; Ren, W. C.; Chen, Z. G.; Tan, J.; Wu, Z. S.; Gentle, I.; Lu, G. Q.; Cheng, H. M. Fabrication of Graphene/Polyaniline Composite Paper via In Situ Anodic Electropolymerization for High Performance Flexible Electrode. *ACS Nano* **2009**, *3*, 1745−1752.
(37) Cong, H. P.; Ren, X. C.; Wang, P.; Yu, S. H. Flexible Graphene−Polyaniline Composite Paper for High Performance Supercapacitor. *Energy Environ. Sci.* **2013**, *6*, 1185−1191.
(38) Wang, L.; Ye, Y. J.; Lu, X. P.; Wen, Z. B.; Li, Z.; Hou, H. Q.; Song, Y. H. Hierarchical Nanocomposites of Polyaniline Nanowire Arrays on Reduced Graphene Oxide Sheets for Supercapacitors. *Sci. Rep.* **2013**, *3*, 3568.
(39) Wang, Y. G.; Li, H. Q.; Xia, Y. Y. Ordered Whiskerlike Polyaniline Grown on the Surface of Mesoporous Carbon and its

Electrochemical Capacitance Performance. *Adv. Mater.* **2006**, *18*, 2619−2623.
(40) Xu, Y. F.; Schwab, M. G.; Strudwick, A. J.; Hennig, I.; Feng, X. L.; Wu, Z. S.; Müllen, K. Screen-Printable Thin Film Supercapacitor Device Utilizing Graphene/Polyaniline Inks. *Adv. Energy Mater.* **2013**, *3*, 1035−1040.
(41) Wang, Y. F.; Yang, X. W.; Qiu, L.; Li, D. Revisiting the Capacitance of Polyaniline by Using Graphene Hydrogel Films as a Substrate: The Importance of Nano-Architecturing. *Energy Environ. Sci.* **2013**, *6*, 477−481.
(42) Gao, H. C.; Xiao, F.; Ching, C. B.; Duan, H. W. Flexible All-Solid-State Asymmetric Supercapacitors Based on Free-Standing Carbon Nanotube/Graphene and Mn_3O_4 Nanoparticle/ Graphene Paper Electrodes. *ACS Appl. Mater. Interfaces* **2012**, *4*, 7020−7026.
(43) Kim, T. Y.; Lee, H. W.; Stoller, M.; Dreyer, D. R.; Bielawski, C. W.; Ruoff, R. S.; Suh, K. S. High-Performance Supercapacitors Based on Poly (ionic liquid)-Modified Graphene Electrodes. *ACS Nano* **2011**, *5*, 436−442.
(44) Cottineau, T.; Toupin, M.; Delahaye, T.; Brousse, T.; Bélanger, D. Nanostructured Transition Metal Oxides for Aqueous Hybrid Electrochemical Supercapacitors. *Appl. Phys. A: Mater. Sci. Process.* **2006**, *82*, 599−606.
(45) Cheng, Y.; Lu, S.; Zhang, H.; Varanasi, C. V.; Liu, J. Synergistic Effects From Graphene and Carbon Nanotubes Enable Flexible and Robust Electrodes for High-Performance Supercapacitors. *Nano Lett.* **2012**, *12*, 4206−4211.
(46) He, Y. M.; Chen, W. J.; Li, X. D.; Zhang, Z. X.; Fu, J. C.; Zhao, C. H.; Xie, E. Q. Freestanding Three-Dimensional Graphene/MnO_2 Composite Networks as Ultralight and Flexible Supercapacitor Electrodes. *ACS Nano* **2013**, *7*, 174−182.